Title
NUMERICAL SOLUTION OF THE PION-PION STRIP-APPROXIMATION N/D EQUATION

Authors
Teplitz, Doris C.
Teplitz, Vigdor L.

Publication Date
1964-07-22

UCRL-11591

University of California

Ernest O. Lawrence Radiation Laboratory

NUMERICAL SOLUTION OF
THE PION-PION STRIP-APPROXIMATION N/D EQUATION

Berkeley, California

DISCLAIMER

UCRL-11591

UNIVERSITY OF CALIFORNIA

Lawrence Radiation Laboratory
Berkeley, California

AEC Contract No. W-7405-eng-48

NUMERICAL SOLUTION OF THE PION-PION STRIP-APPROXIMATION N/D EQUATION

Doris C. Teplitz and Vigdor L. Teplitz

July 22, 1964

NUMERICAL SOLUTION OF THE PION-PION STRIP-APPROXIMATION N/D EQUATION*

Doris C. Teplitz

Oakland, California

and

Vigdor L. Teplitz

Lawrence Radiation Laboratory
University of California
Berkeley, California

July 22, 1964

ABSTRACT

Chew's strip-approximation N/D equations have been solved numerically with a generalized potential of the form corresponding to elementary particle ρ exchange plus the contribution from Pomeranchon exchange required by the fact that the phase shift at the strip boundary is generally nonzero. Trajectories and reduced residue functions are found. The trajectories have reasonable shapes, slopes in agreement with experiment $[\alpha' \approx 0.3/(\mathrm{BeV}/c)^2]$ for reasonable chosen strip widths, and end points in the region of $\ell \gtrsim 0$. Increasing the phase shift at the strip boundary displaces trajectories upward, while increasing the strip width tends to flatten trajectories. The behavior of the reduced residues is found to be representable by a simple approximate formula in terms of the input potential. The potential investigated, with neglect of inelastic scattering, is incapable of generating a $J = 2$, $I = 0$ resonance and yields a ρ width several times too large. Increasing the phase shift at the strip boundary tends to improve the situation.

I. INTRODUCTION

Chew[1,2] and Chew and Jones[3] have recently proposed a new method of solving the pion-pion problem, based on the strip approximation.[4] The starting point in the calculation they propose consists of trajectories and reduced residue functions in the crossed channel, and the width of the strip inside which the double-spectral functions are nonnegligible. Chew and Jones have shown how to obtain from these quantities a Born term which includes the effects of resonance exchange, continuum exchange, and inelastic processes in the direct channel.[3] Chew has given the solution of the resulting (non-Fredholm) modified integral equation for $N_\ell(s)$.[2] An iterative procedure is envisioned in which self-consistent solutions are found such that the output trajectories and residues are identical to the input ones. The purpose of this paper is to give numerical results for the solution of the modified integral equation when the Born term is approximated by the exchange of a zero-width ρ. We feel these results are of interest both as a starting point with which to compare the more inclusive calculation in progress and as an indication of the size of the role played by ρ exchange in the pion-pion problem. No attempt is made in the present work to find self-consistent solutions. We rather study the output trajectories and residues as functions of the width of the exchanged ρ, the strip boundary, and the phase shift at the strip boundary. Our results, briefly, with strip widths around 5 GeV^2 are leading trajectories, α, of reasonable $\alpha'(0)$ [around $0.3/(\text{BeV}/c)^2$] and reasonable $\alpha(\infty)$ [$0 < \alpha(\infty) < 0.5$], and reduced residue functions, γ, in agreement with the approximation of Chew and Teplitz,[5]

$$\gamma(s)/\alpha'(s) = (\bar{s} - s)B^V_{\alpha(s)}(\bar{s}) , \quad \text{for} \quad s \ll \bar{s} ,$$

where $\bar{s}$ is in the strip and B^V is the potential. The Pomeranchuk trajectory cannot be made to reach $J = 2$ with the potential in question, and the residue at $s = m_\rho^2$ for $\alpha(m_\rho^2) = 1$ is several times as large as the value corresponding to the observed ρ width. In Section II we review the equations to be solved and discuss the machine program which solves them. In Section III we give the Born term. In Section IV we present our results; and finally, in Section V we briefly discuss corrections to the Born term.

II. N/D EQUATIONS

Chew's equations are[2]

$$D = 1 - \pi^{-1} \int_4^{s_1} \rho_\ell(s')N_\ell(s')/(s' - s) , \tag{1}$$

$$N_\ell(s) = \int_4^{s_1} O_\ell(s,s')N^O_\ell(s') , \tag{2}$$

$$N^O_\ell(s) = B^V_\ell(s) + \int_4^{s_1} ds' K'_\ell(s,s')N^O_\ell(s') , \tag{3}$$

$$K'_\ell(s,s') = \int_4^{s_1} K_\ell(s,s'')O_\ell(s'',s')ds'' , \tag{4}$$

and $K_\ell(s,s') = [\pi(s'-s)]^{-1}\{[B_\ell^V(s') - B_\ell^V(s)]\rho_\ell(s')$

$$+ (\lambda_\ell/\pi)[\ell n(s_1 - s') - \ell n(s_1 - s)]\}, \quad (5)$$

where $\lambda_\ell = \sin^2 \pi a_\ell$, $\pi a_\ell = \delta_\ell(s_1)$. Here O_ℓ is given by

$$O_\ell(s,s') = \delta(s'-s) + \tan \pi a_\ell O_A(s,s') - \tan^2 \pi a_\ell O_B(s,s'), \quad (6)$$

with

$$O_A(s,s') = (2\pi)^{-1}\{[(s_1 - s')/(s_1 - s)]^{a_\ell} - [(s_1 - s)/(s_1 - s')]^{a_\ell}\}/[s'-s]. \quad (7)$$

The O_B has been written down explicitly;[6] it is a double summation and positive, and less than O_A for $a_\ell < 1/2$.

As Chew has pointed out,[2] we may see from Eq. (7) that $N_\ell(s)$ and $D_\ell(s)$ are both singular at the strip boundary s_1, behaving like $(s_1 - s)^{-a_\ell}$; the singularity is not, however, present in the amplitude $B_\ell(s)$. We also recall that ℓ is the end point of a trajectory if Eq. (3) has a homogeneous solution.[3]

The solution of Eqs. (1) through (5) has been programmed for the IBM 7094 computer. The input to the program consists of s_1, ℓ, a_ℓ, and $B_\ell^V(s)$; the output [in addition to $N_\ell(s)$ and $D_\ell(s)$] consists of the resonance energies $s_R(\ell)$ and the quantity $\gamma(s)/\alpha'(s)$ [which is equal to $N_\ell(s)/(dD_\ell(s)/ds)$]. Integrations are done by Gaussian quadratures applied to the variable $(s_1 - s)^{\frac{1}{2}}$ because of the singular behavior at s_1. The Fredholm equation (3) is solved by matrix inversion, again using Gaussian quadratures in approximating the integral operator by a matrix operator. As we shall see below, B_ℓ^V for ρ exchange is rather smoothly varying. As a result the matrix in Eq. (3) yields results (resonance energies and widths) when it is 15 by 15 that are within 1% of the results for 40 by 40. About 50% of the running time for the program is used in computing the operator $O_\ell(s,s')$ for Eqs. (2) and (4); 100 to 400 terms in the double sums for O_B are used, depending on the sizes of s and s'. Finding s_R and γ/α' from the input takes about 25 seconds.

III. THE GENERALIZED POTENTIAL

In this work we have used for the generalized potential

$$\begin{Bmatrix} B_\ell^{V,T=0}(s) \\ B_\ell^{V,T=0}(s) \\ B_\ell^{V,T=2}(s) \end{Bmatrix} = B_\ell^P(s) + B_\ell^\rho(s) \quad , \tag{8}$$

where for the ρ contribution we take

$$B_\ell^\rho(s) = \begin{Bmatrix} 1 \\ \frac{1}{2} \\ -\frac{1}{2} \end{Bmatrix} (3\Gamma_\rho \sqrt{t_\rho}/q_s^{2\ell+2})(1 + s/2q_\rho^2)Q_\ell(1 + t_\rho/2q_s^2) \quad , \tag{9}$$

with Γ_ρ the full width in the energy at half maximum, while for the Pomeranchon trajectory contribution we take

$$B_\ell^P(s) = -\begin{Bmatrix} 1 \\ 1 \\ 1 \end{Bmatrix} \left(\frac{\sin^2 \pi a_\ell}{\pi \rho_\ell(s_1)} \right) \ln[(s_1 - s)/s_1] \quad . \tag{10}$$

Equation (10) represents only the portion of the Pomeranchon contribution to the potential which is singular at s_1. We include this part in order to study numerically the dependence of the solution to Eqs. (1) through (5) on the condition at the strip boundary. The interpretation of this term is that it gives the contribution to the potential from inelastic processes in the direct channel above s_1. Except for s very near s_1 we have $B_\ell^P \ll B_\ell^\rho$, and the subtraction of the logarithmic terms in (5) makes the kernel $K_\ell(s, s'')$ almost independent of the Pomeranchon potential

The ρ contribution [Eq. (9)] has several interesting features: (a) In studying the output trajectories as a function of the input width Γ_ρ, the T = 0 trajectories with input Γ_ρ are identical to the T = 1 trajectories with $2\Gamma_\rho$ as input. (b) For $\ell = 1$, $B_\ell^\rho(s)$ rises slightly from s = 4 to s = $2t_\rho$ and then falls very gently; it is constant to about 20% up to s values around 300 m_π^2. From Eq. (5) we see that the constancy of B_ℓ^ρ and the smallness of B_ℓ^P, except very near s_1, imply that the kernel of the Fredholm equation (3) is small. Thus the Born term is a good approximation to the solution for N^0, and hence for N. (c) As ℓ increases from 1, $B_\ell^\rho(s)$ becomes a more strongly decreasing function of s and the integral term in Eq. (3) yields consequently a larger repulsive contriubtion.

(d) As ℓ decreases from 1 the opposite obtains; $B_\ell^\rho(s)$ becomes an increasing function and the integral term an attraction. Property (c) tends to limit the maximum value of ℓ that may be attained by a trajectory. For reasonable input widths, the output trajectories tend to turn over in the neighborhood of $\ell = 1$ or below. For very large input widths the output trajectories may be forced to somewhat higher maxima, but then $\alpha(\infty)$ rises correspondingly by property (d).

IV. RESULTS AND DISCUSSION

In Figures 1 through 9 we show a series of trajectories for different values of a_ℓ, Γ, and s_1, found from setting Re $D_\ell(s) = 0$. In the figures the values of Γ are appropriate to the $T = 1$ direct channel; a $T = 0$ trajectory for given Γ may be read from the figure of the $T = 1$ trajectory for 2Γ. In plotting the trajectories, a_ℓ has been assumed constant in ℓ. Clearly an increasing a_ℓ yields a trajectory with greater slope, and a decreasing a_ℓ lesser slope. We recall that the strip boundary s_1 is expected to be large enough so that a_ℓ [which is $= \delta(s_1)/\pi$] is less than 1/2. The values chosen for the strip boundary s_1 are reasonable in that they are above the highest $\pi\pi$ resonance (the f_o at $s = 80\ m_\pi^2$) but not high enough to be in the region in which Regge behavior seems to become valid for πN and NN ($s \approx 500\ m_\pi^2$).

Only the parts of the trajectories for which $\alpha(s)$ is rising from $\alpha(-\infty)$ are shown, since for s above this range, Im α is presumably too large for the interpretation of ℓ as Re α from Re $D_\ell(s) = 0$. For the same reason the maximum value reached by a trajectory is indicated, but the detailed shape near this value is not given. The maximum slopes of the trajectories shown lie in the range $0.1/(50\ m_\pi^2) - 0.6/(50\ m_\pi^2)$, which brackets the values obtained for the slopes of boson trajectories from fitting high-energy data[7] $[\alpha' \approx 0.3/(50\ m_\pi^2)]$. The values of $\alpha(\infty)$ are all above 0 for the cases shown. If this feature persists with better Born terms it will provide a dynamical resolution of the problem of the s-wave Pomeranchon ghost. The most striking drawback in the trajectories shown is that they all turn over well under $\ell = 2$, as discussed in Section III. Thus, while ρ exchange accounts qualitatively for the existence of the ρ, it is inadequate for an understanding of the f_o. A second, possibly difficult, feature of the results is that secondary trajectories (S) were found to lie completely under the primary trajectories (T), i.e., $\alpha_S^{max} < \alpha_T(\infty)$.

We may also see, from Figs. 1 - 5 and 6 - 7, that increasing a_ℓ and Γ tends to raise trajectories in an approximately paralllel manner. A more detailed picture of the dependence of $s_R(\ell)$ on a_ℓ is shown in Fig. 10 for a case of ℓ, near the trajectory maxima, for which the resonance energy is particularly sensitive to a_ℓ. It should be noted that $s_R(\ell)$ behaves smoothly in the limit $a_\ell \to \frac{1}{2}$.[6] With respect to the strip width, we see from Figs. 8 and 9 that increasing s_1 tends to raise and flatten trajectories. A measure of the flattening can be found from the approximation, for $s < 0$,

$$\alpha(s) = \alpha(\infty) + [\alpha(0) - \alpha(\infty)]/(1 - 2s/s_1)$$

which seems to fit the trajectories fairly well.

Three other calculations of $\alpha(s)$ may be compared with the above results. Bransden et.al.[8] have computed leading trajectories from the original form of the Chew-Frautschi[4] strip approximation, in which unitarity is applied to the full amplitude rather than to partial waves. They find also that the exchange force cannot yield a trajectory rising to $\ell = 2$. For strip widths in the range $100 < s_1 < 200\ m_\pi^2$, they find trajectory slopes of about $0.3/(\mathrm{BeV}/c)^2$, in agreement with the results presented above. Bander and Shaw[9] have calculated trajectories, using the N/D method and a generalized potential suggested by Wong.[10] Although their work is not within the strip approximation, their result for trajectory slopes was roughly very small slopes, $\alpha' < 0.05/(\mathrm{BeV}/c)^2$, for very large strip widths, $s_1 > 1000\ m_\pi^2$. Finally, Igi[11] has computed $\alpha'(0)$ in the strip-approximation N/D formulation of Balazs,[12] and has seen the flattening of trajectories as the strip boundary varies from 80 to 160 m_π^2. Igi's values for $\alpha'(0)$ are somewhat larger than those obtained above, but this is a result of the inclusion of some inelasticity below the strip boundary.

Our results for the reduced residue functions $\gamma(s)$ are in agreement with the approximation of reference 5,

$$\gamma(s)/\alpha'(s) = -\int_4^{s_1} (s' - s)^{-1} \rho_\ell N_\ell B_\ell^V \bigg/ \int_4^{s_1} (s' - s)^{-2} \rho_\ell N_\ell$$

$$\approx (\bar{s} - s) B^V_{\alpha(\bar{s})}(\bar{s}) \quad ,$$

for $\alpha(s)$ sufficiently far from its maximum $[\alpha_{max} - \alpha(s) > 0.1]$. For larger $\alpha(s)$, γ/α' [which equals N/D'] falls below this approximation, but as s approaches $s_R(\alpha_{max})$, becomes infinite. In Fig. 11 we show, as an example, $\gamma(s)$ for a trajectory of Fig. 4 with $\bar{s} = s_1/2$. This case ($\Gamma = 2$) corresponds, in the T = 0 channel, to an exchanged ρ of the experimental width (140 MeV) and has $\alpha(0) \approx 1$. If we compute the pion-pion total cross section from the formula,

$$\sigma_{\pi\pi} = 8\pi^2\lambda(0)$$

using $\gamma/\alpha' \approx 3$ from Fig. 11 and $\alpha' \approx 1/100\ \mu^2$ from Fig. 8, we find $\sigma_{\pi\pi} \approx 50$ mb. This result is three to five times as large as the values deduced from the factorization principle[13] and the πN and NN cross sections. The fact that γ is too large seems to be connected with the fact that α_{max} is too small through the observation that both difficulties would be eased if the integral term in Eq. (3) gave a sizable attractive contribution for $\ell = 1$. In such a case the trajectory would rise higher, since α_{max} is determined by the point at which the integral term becomes repulsive; $\gamma(0)$ would be smaller since by Eq. (1) it is proportional to B^V, which is N less the integral term. A similar situation obtains for an output ρ which is always too broad.[14] Thus the principal deficiencies of elementary ρ exchange seem to stem from the lack of attraction from the integral term in Eq. (3) which, in turn, may be attributed to the constant, for $\ell = 1$, behavior of the potential discussed in Section III. Since this behavior results from the fixed spin (=1) of the exchanged ρ we may expect some improvement in a calculation in which the Regge behavior of the exchanged ρ is included.

V. CORRECTIONS TO THE GENERALIZED POTENTIAL

We review here the changes, within the strip approximation, expected in a calculation of the generalized potential $B_\ell^V(s)$ more accurate than the δ-function ρ approximation used above.

(i) Regge behavior of the ρ:[1,3] the contribution to $A(s,t)$ from an elementary t channel ρ,

$$A^\rho(s,t) \propto \Gamma P_1(z_t)/(t_\rho - t) ,$$

is only an approximation to the contribution from a ρ trajectory,

$$A^\rho(s,t) \sim (2\alpha + 1)(-q_t^2)^{\alpha(t)}\gamma(t)P_{\alpha(t)}(z_t)/\sin \pi\, \alpha(t) + \ldots .$$

The first form is recaptured from the second in the limit $\alpha \to 1 + \epsilon(t - t_R)$, $\gamma \to \epsilon$, $\epsilon \to 0$. The modifications introduced by the Regge form are currently being studied numerically.

(ii) The contribution of the Pomeranchon trajectory (P): in addition to the logarithmically (at $s = s_1$) singular part considered above, there is another contribution to the amplitude due to the P and secondary T = 0 trajectories that come to the right of $\ell = -\frac{1}{2}$, which can be written[15]

$$A^{T=0}(s,t) \sim \sum_\ell (2\ell + 1) \int dt' \sigma^{T=0}(t')/(t' - t) + \ldots .$$

In view of the nonresonant behavior of the s wave and the high mass of the f_0 in the d wave, this term is very likely unimportant.

(iii) The double-spectral functions with support in the region of low s and large t: these give a contribution to the left-hand cut of $A(s,t)$ which must be included in finding B_ℓ^V (in addition to their contribution to the right-hand cut of $A(s,t)$ which is being solved for and is not to be included in B_ℓ^V).[3] The left-hand cut from this term begins, however, at $s = -s_1$, so that this term is presumably small for the same reasons as those which justify the strip approximation.

(iv) Inelastic channels below the strip boundary such as $\pi\omega$, $\rho\rho$, and $K\bar{K}$: two possible methods for finding their effects are: (a) a multichannel calculation and (b) introduction of the inelasticity parameter $R_\ell(s) = \sigma^T(s)/\sigma^{E\ell}(s)$ into the equations of Section II. It has been pointed out that (b) is easily accomplished by replacing $\rho_\ell(s)$ by $\rho_\ell(s)R_\ell(s)$; but reliabily calculating, or even estimating, $R_\ell(s)$ does not, at present, appear feasible.[6] The absence of any four-pion decay of the f_0, however, lends support to the neglect of inelastic effects below the strip boundary.

The qualitative success of the simple δ-function exchange contribution in yielding Regge trajectories of reasonable shape and reduced residue functions of reasonable magnitude gives some encouragement that the inclusion of (i), and possibly others, above will make it possible to find a solution to the pion-pion bootstrap equations.

ACKNOWLEDGMENT

We are grateful to Professor Geoffrey F. Chew for many helpful discussions. One of us (V.L.T.) wishes to thank Dr. David L. Judd for his hospitality at the Lawrence Radiation Laboratory.

REFERENCES

* This work was done under the auspices of the United States Atomic Energy Commission.

1. G. F. Chew, Rev. 129, 2363 (1963).
2. G. F. Chew, Rev. 130, 1264 (1963).
3. G. F. Chew and C. E. Jones, Phys. Rev. 134, B208 (1964).
4. G. F. Chew and S. C. Frautschi, Phys. Rev. 124, 264 (1961).
5. G. F. Chew and V. L. Teplitz, Dynamical Formula for the Slope of the Pomeranchuk Trajectory, Lawrence Radiation Laboratory Report UCRL-11495, July 1964 (submitted to Phys. Rev.).
6. V. L. Teplitz, Solution of the N/D Equations in the Strip Approximations, Lawrence Radiation Laboratory Report UCRL-11555, July 1964 (submitted to Phys. Rev.).
7. A. Ahamadzadeh and I. Sakmar, Physics Letters 5, 145 (1963); Phys. Rev. Letters 9, 459 (1963); B. Desai, Phys. Rev. Letters 11, 59 (1963); W. Rarita and V. Teplitz, Phys. Rev. Letters 12, 206 (1964).
8. H. Bransden, P. G. Burke, J. W. Moffat, R. G. Moorhouse, and D. Morgan, Nuovo Cimento 30, 207 (1963).
9. M. Bander and G. L. Shaw, Phys, Rev. 134, B267 (1964).
10. D. Wong, Phys. Rev. 126, 1220 (1962).
11. K. Igi, Self-Consistent Calculation of the Scattering Amplitude and the Diffraction Peak, Institute for Advanced Study preprint, May 1964 (to be published).
12. L. A. P. Balazs, Phys. Rev. 132, 867 (1963).

13. M. Gell-Mann, Phys. Rev. Letters 8, 263 (1962);

V. Gribov and I. Pomeranchuk, Phys. Rev. Letters 8, 343 (1962).

14. This is a well-known feature of pion-pion calculation. See, for example, reference 9.

15. G. F. Chew and V. L. Teplitz, A more Accurate Treatment of the Low-Energy Potential in the Strip Approximation, Lawrence Radiation Laboratory Report UCRL-11370 April 1964 (unpublished).

FIGURE CAPTIONS

Fig. 1. $\alpha(s)$ for $\Gamma = 1$, $s_1 = 200$, $a_\ell = 0.1, 0.3$.

Fig. 2. $\alpha(s)$ for $\Gamma = 2$, $s_1 = 100$, $a_\ell = 0.1, 0.3$.

Fig. 3. $\alpha(s)$ for $\Gamma = 2$, $s_1 = 200$, $a_\ell = 0.1, 0.3$.

Fig. 4. $\alpha(s)$ for $\Gamma = 2$, $s_1 = 300$, $a_\ell = 0.1, 0.3$.

Fig. 5. $\alpha(s)$ for $\Gamma = 4$, $s_1 = 200$, $a_\ell = 0.1, 0.3$.

Fig. 6. $\alpha(s)$ for $a_\ell = 0.1$, $s_1 = 200$, $\Gamma = 1, 2, 4$.

Fig. 7. $\alpha(s)$ for $a_\ell = 0.3$, $s_1 = 200$, $\Gamma = 1, 2, 4$.

Fig. 8. $\alpha(s)$ for $a_\ell = 0.1$, $\Gamma = 2$, $s_1 = 100, 200, 300$.

Fig. 9. $\alpha(s)$ for $a_\ell = 0.3$, $\Gamma = 2$, $s_1 = 100, 200, 300$.

Fig. 10. $s_R(a_\ell)$ for $\Gamma = 1$, $s_1 = 200$, $\ell = 1.0$.

Fig. 11. Numerical results for $\gamma(s)/\alpha'(s)$ solid curve; the approximation of reference 5 dotted curve, for $\Gamma = 2$, $s_1 = 300$, $a_\ell = 0.3$.

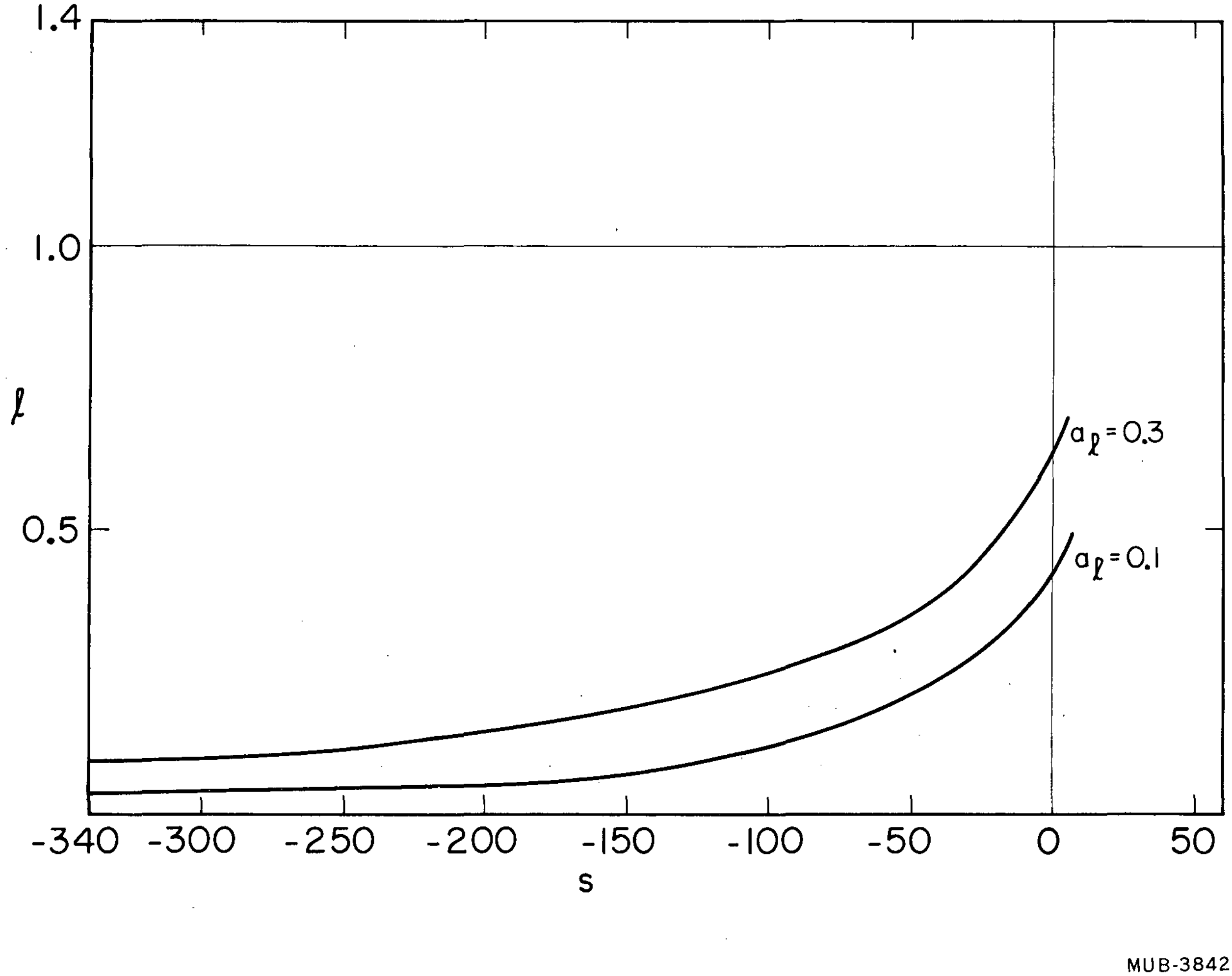
1.4
1.0
0.5
ℓ
$a_\ell = 0.3$
$a_\ell = 0.1$
-340 -300 -250 -200 -150 -100 -50 0 50
s
MUB-3842

Fig. 1

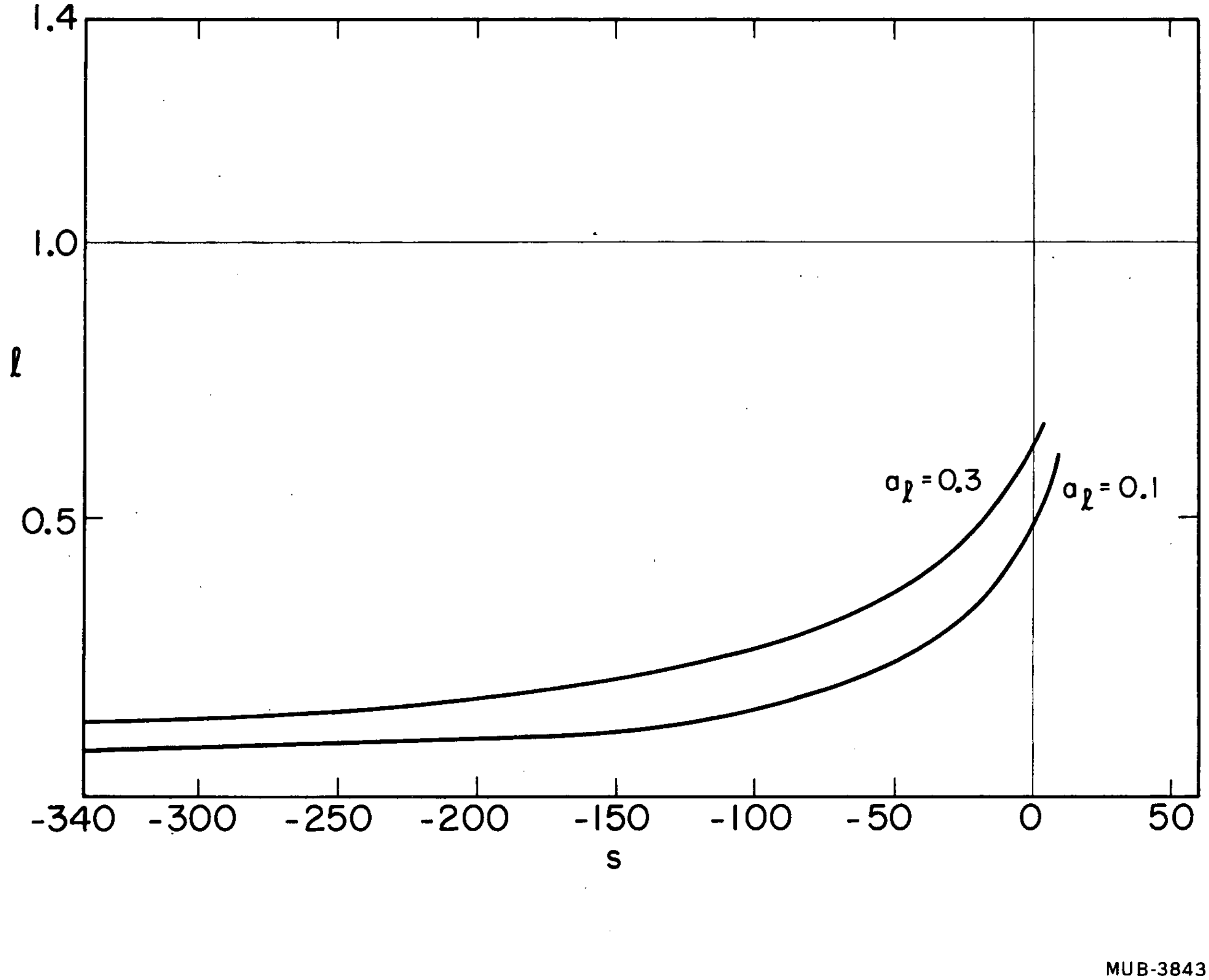
1.4
1.0
0.5
ℓ
$a_\ell = 0.3$
$a_\ell = 0.1$
-340 -300 -250 -200 -150 -100 -50 0 50
S
MUB-3843

Fig. 2

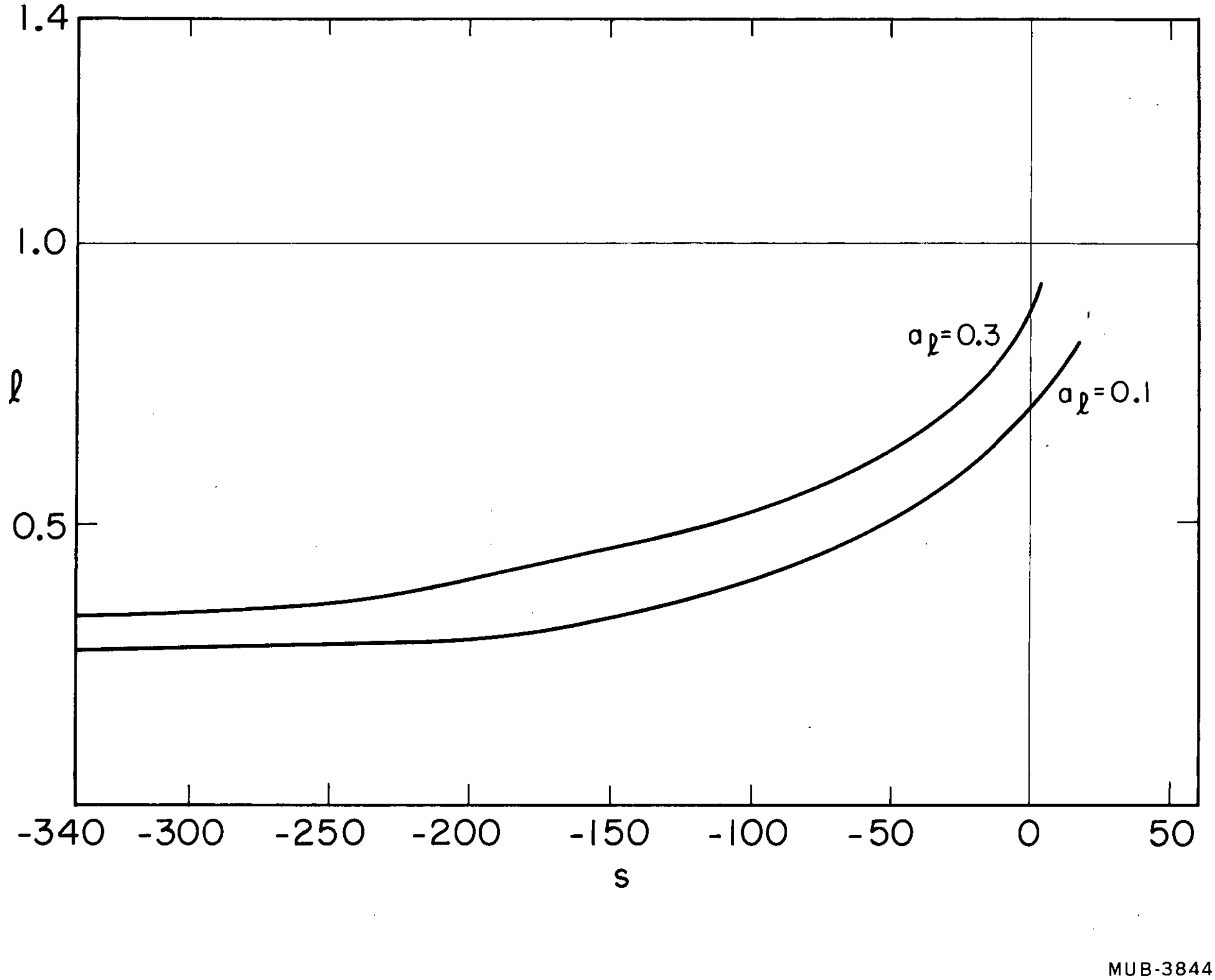
1.4
1.0
0.5
ℓ
$a_\ell = 0.3$
$a_\ell = 0.1$
-340
-300
-250
-200
-150
-100
-50
0
50
s
MUB-3844

Fig. 3

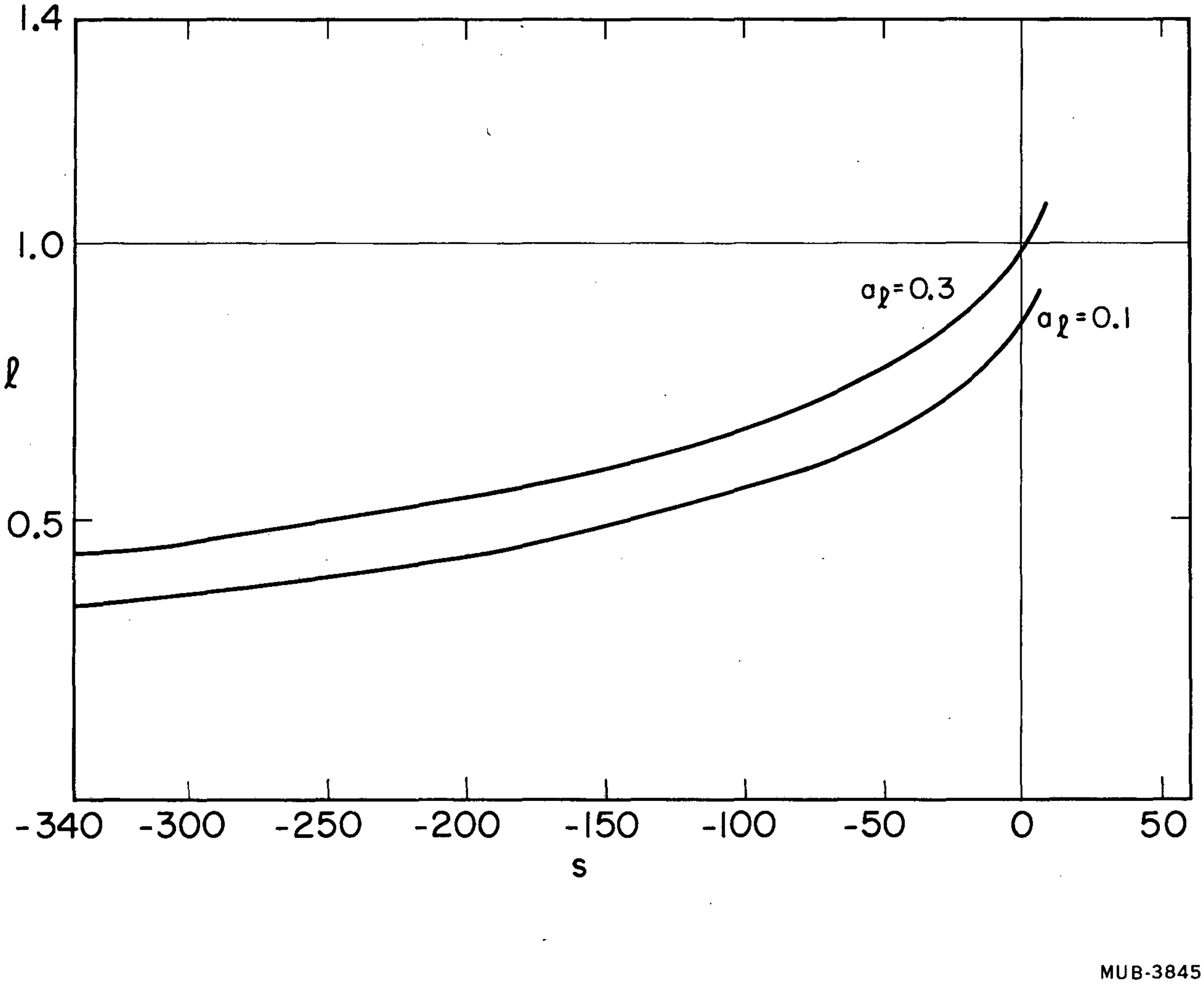
1.4
1.0
0.5
ℓ
$a_\ell = 0.3$
$a_\ell = 0.1$
-340 -300 -250 -200 -150 -100 -50 0 50
s
MUB-3845

Fig. 4

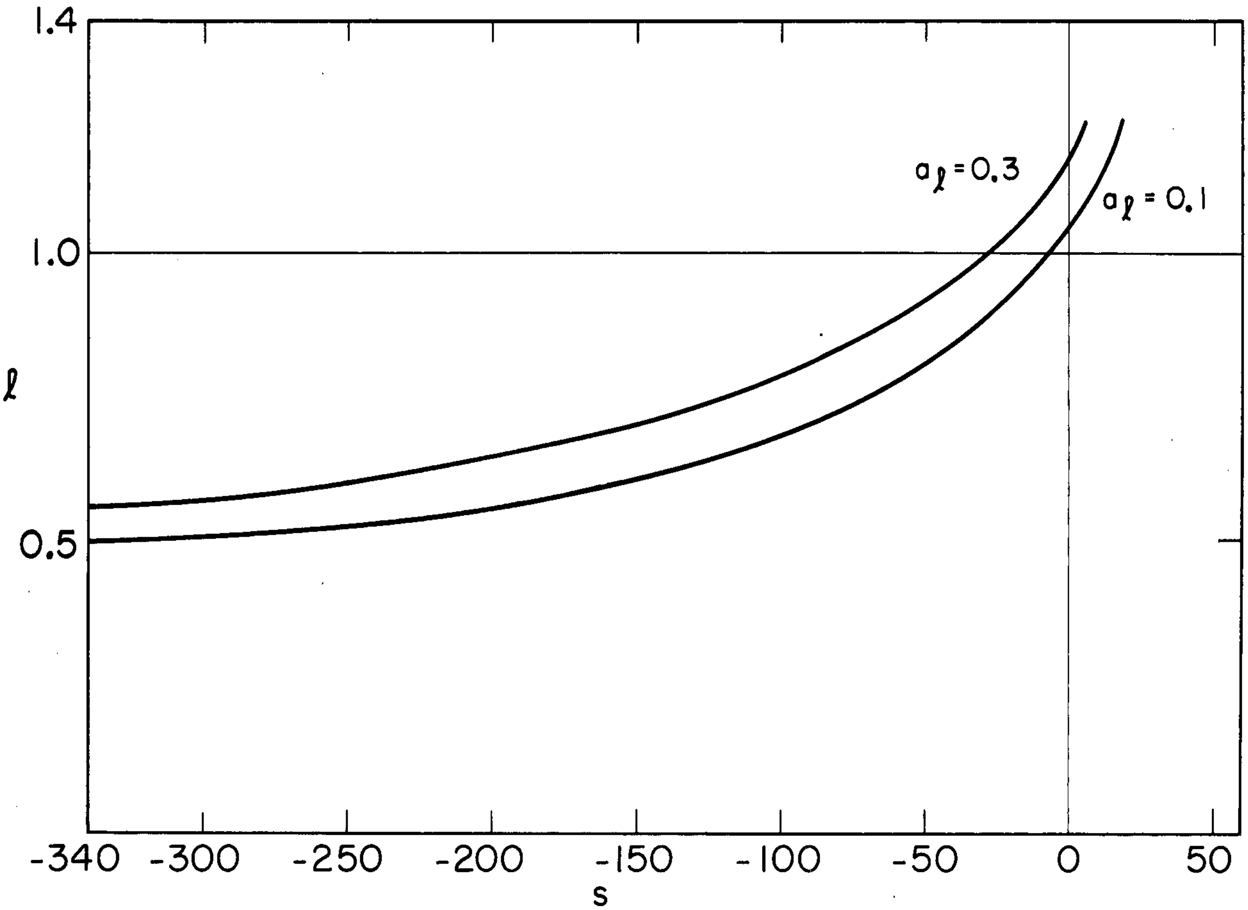

MUB-3846

Fig. 5

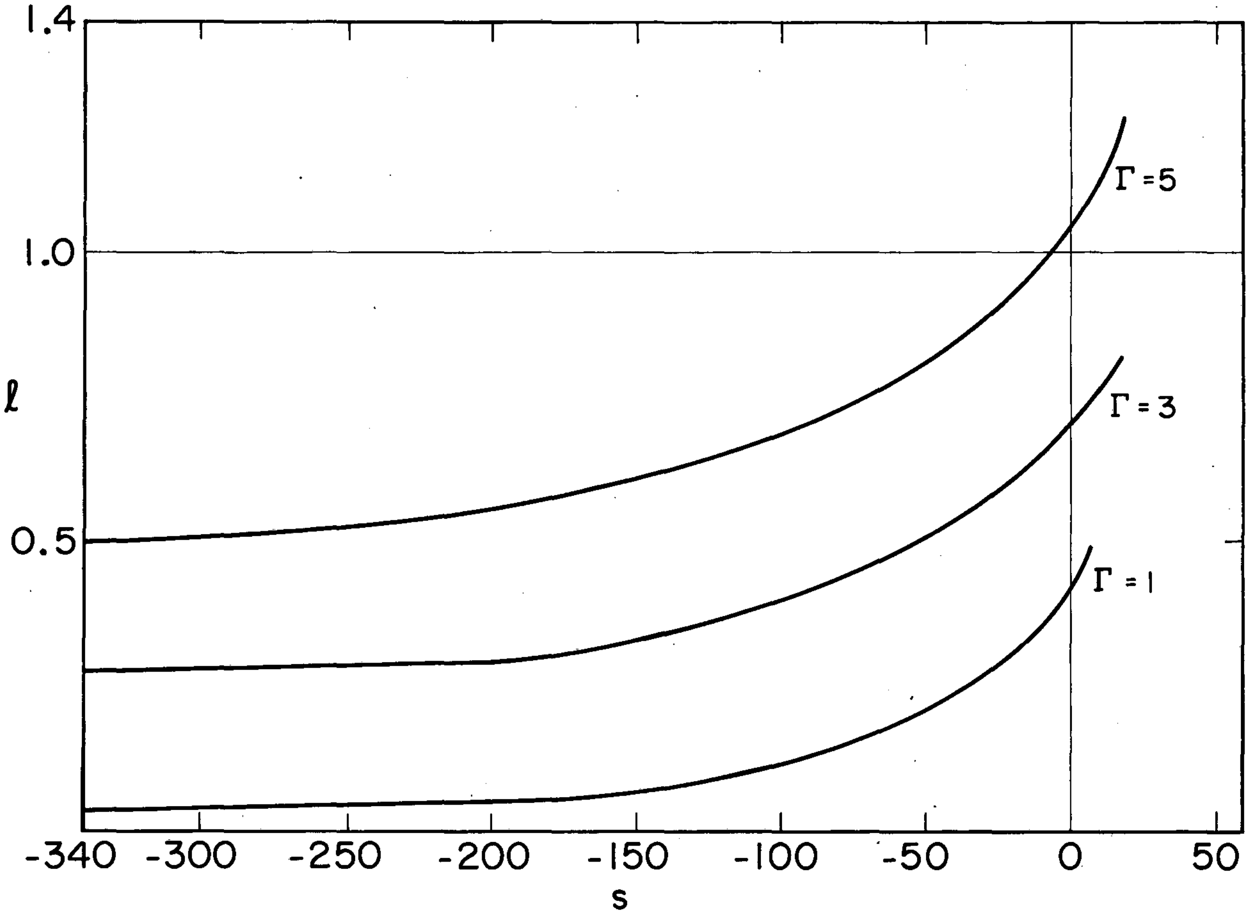

Fig. 6

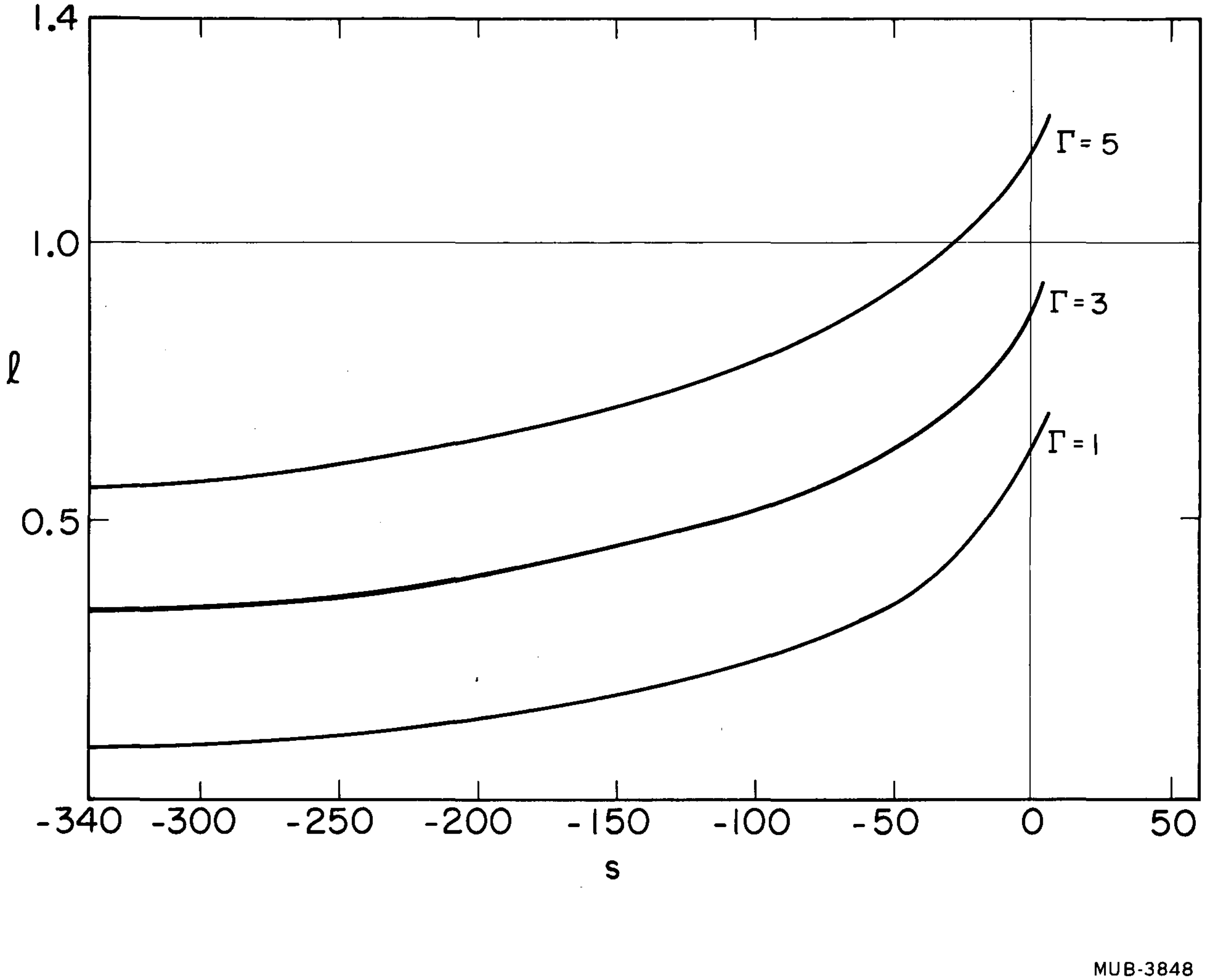

Fig. 7

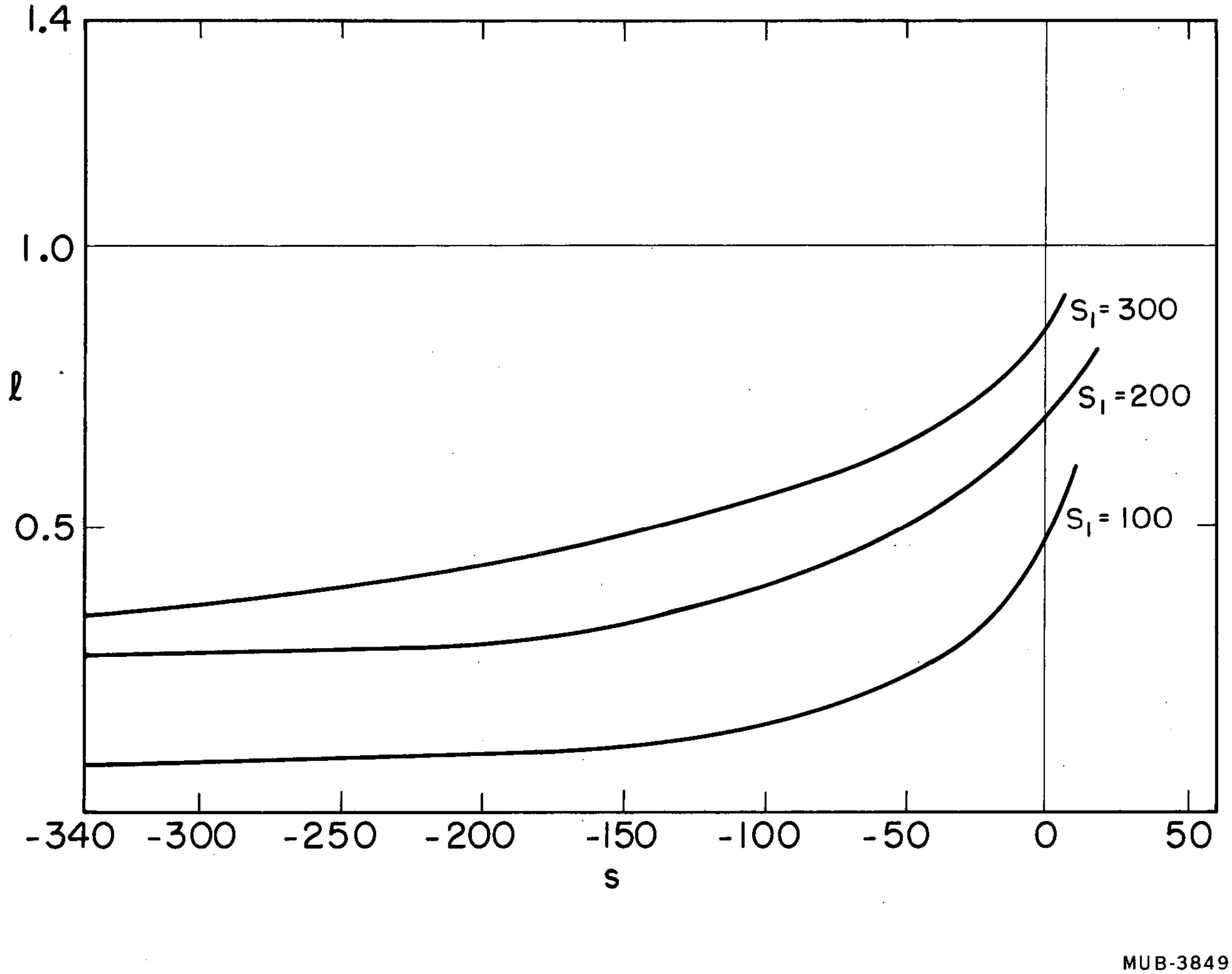
1.4
1.0
0.5
ℓ
$S_1 = 300$
$S_1 = 200$
$S_1 = 100$
-340 -300 -250 -200 -150 -100 -50 0 50
s
MUB-3849

Fig. 8

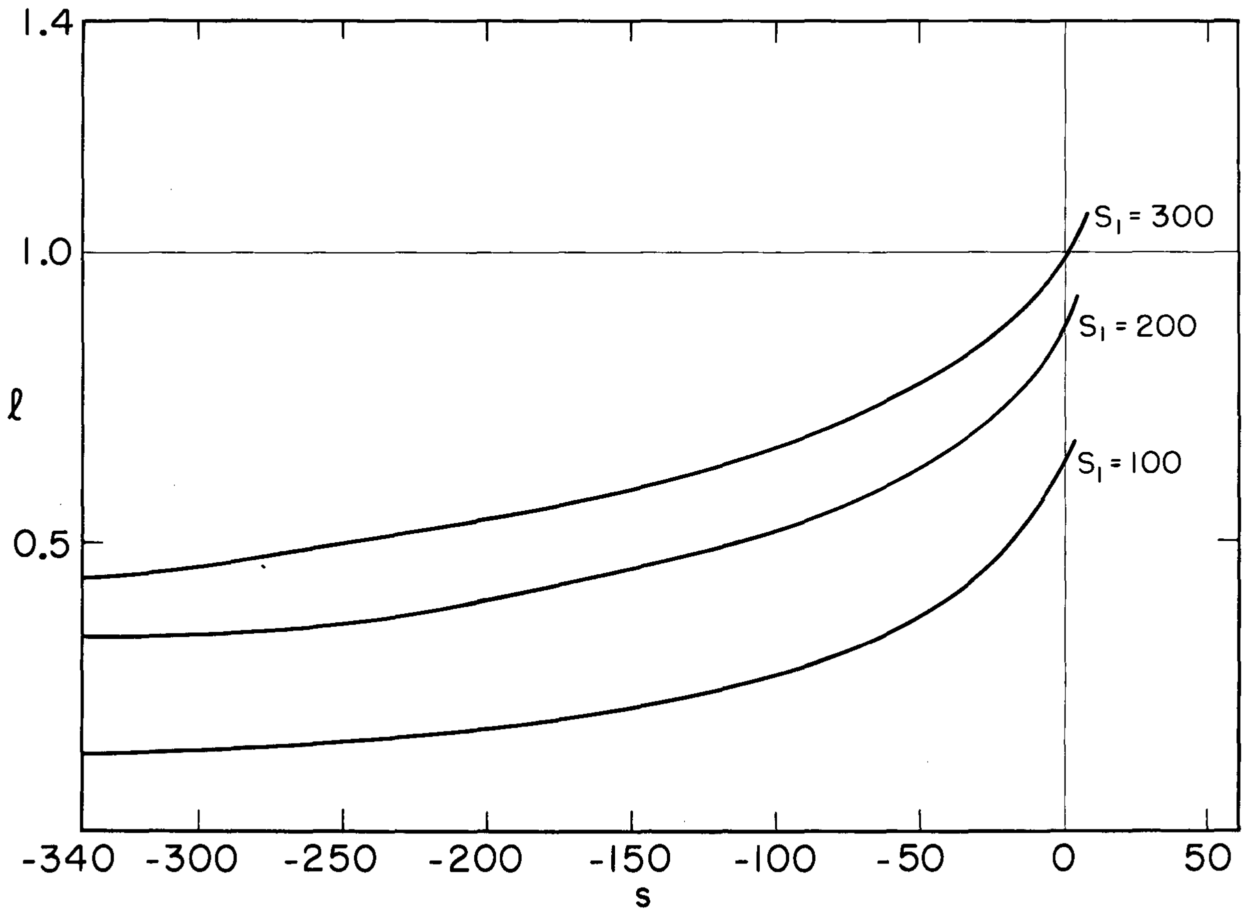

MUB-3850

Fig. 9

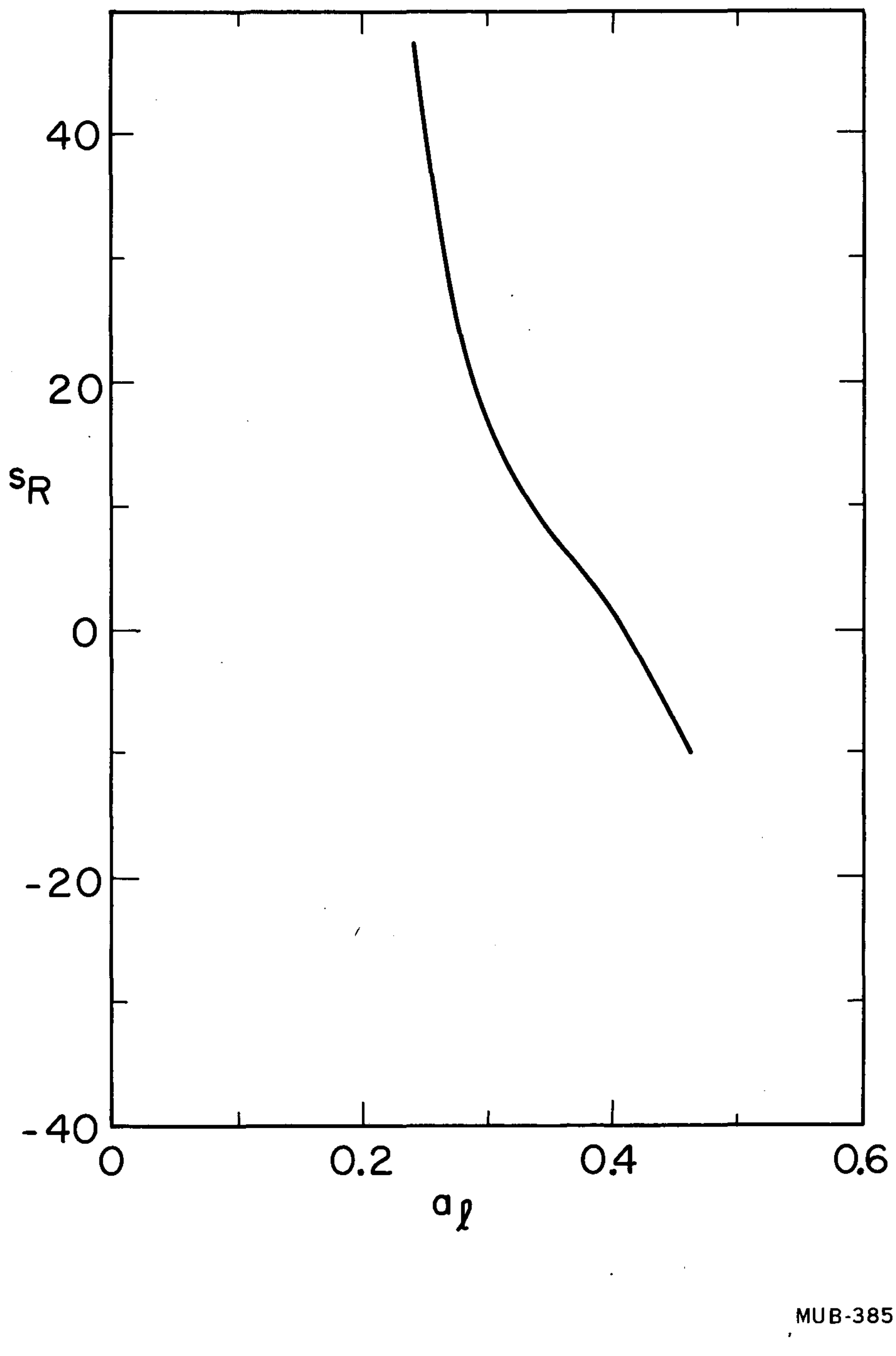

Fig. 10

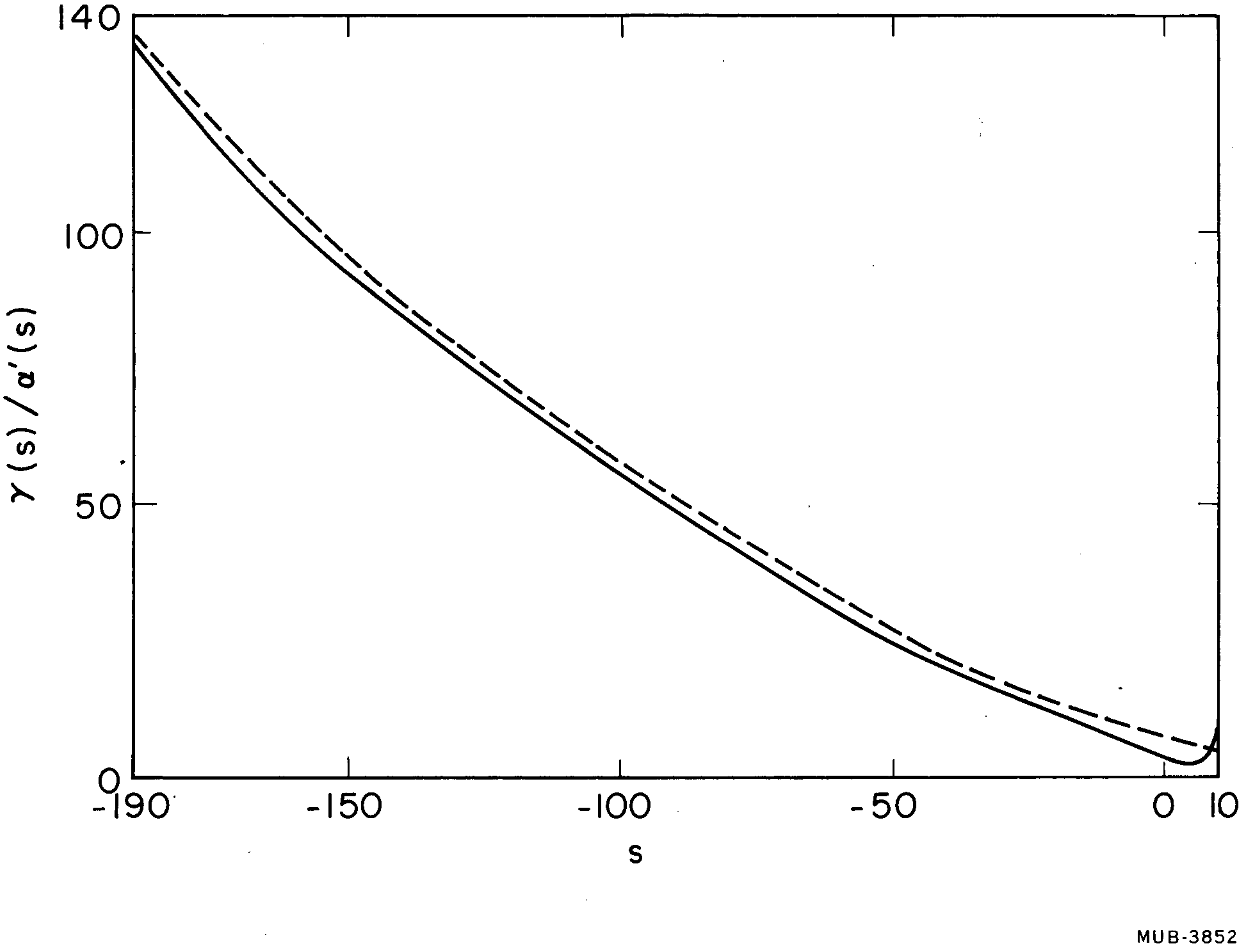

Fig. 11